Journal of Zhejiang University-SCIENCE B (Biomedicine & Biotechnology)
ISSN 1673-1581 (Print); ISSN 1862-1783 (Online)
www.jzus.zju.edu.cn; www.springerlink.com
E-mail: jzus@zju.edu.cn

Central visual function and inner retinal structure in primary open-angle glaucoma*

Li-juan XU[1,2], Sha-ling LI[1], Vance ZEMON[3], Yan-qian XIE[1], Yuan-bo LIANG[†‡1,4]

[1]*Clinical and Epidemiological Eye Research Center, Eye Hospital, School of Optometry and Ophthalmology, Wenzhou Medical University, Wenzhou 325027, China*

[2]*Department of Ophthalmology, Sir Run Run Shaw Hospital, School of Medicine, Zhejiang University, Hangzhou 310016, China*

[3]*Ferkauf Graduate School of Psychology, Albert Einstein College of Medicine Campus, Yeshiva University, New York 10461, USA*

[4]*Global Eye Health, Centre for Public Health, Queens University, Belfast BT71NN, UK*

[†]E-mail: yuanboliang@126.com

Received Aug. 29, 2019; Revision accepted Jan. 7, 2020; Crosschecked Mar. 11, 2020

Abstract: To investigate associations between central visual function and inner retinal structure in primary open-angle glaucoma (POAG). This study enrolled 78 POAG patients and 58 healthy controls. POAG was classified into early glaucoma and moderate to advanced glaucoma. The following tests were performed on all participants: isolated-check visual evoked potential (icVEP) testing, 24-2 standard automated perimetry (SAP), and Cirrus optical coherence tomography (OCT) examinations. Signal-to-noise ratio (SNR) measures obtained from icVEP responses to isolated checks presented at four depths of modulation (DOMs; 8%, 14%, 22%, and 32%) were explored. Mean macular sensitivity (mMS) was assessed by calculating the mean sensitivities of central 12 SAP points. Ganglion cell layer+ inner plexiform layer thickness (GCL+IPLT) and peripapillary retinal nerve fiber layer thickness (pRNFLT) were measured by OCT scanning. For each group of subjects, linear relationships among the following measures were analyzed: SNR, mMS, GCL+IPLT, and pRNFLT. SNR, mMS, GCL+IPLT, and pRNFLT were all more significantly decreased in glaucoma than in controls (P<0.001). A significant positive association was found between SNR at 14% DOM and GCL+IPLT at the inferior sector in early glaucoma (r=0.465, P=0.004). In moderate to advanced glaucoma, significant correlations were found between SNR at 32% DOM and mean GCL+IPLT (r=0.364, P=0.023), superior GCL+IPLT (r=0.358, P=0.025), and mean pRNFLT (r=0.396, P=0.025). In addition, in moderate to advanced glaucoma, there were significant correlations between mMS and all relevant measures of retinal thickness (r=0.330–0.663, P< 0.010). In early glaucoma, significant correlations were found between mean mMS and minimum GCL+IPLT (r=0.373, P=0.023), and between inferior mMS and superior GCL+IPLT (r=0.470, P=0.003). Linear models provided a good explanation for the relationship between SNR and inner retinal thickness (IRT), whereas nonlinear models better explained the relationship between mMS and IRT. In early glaucoma, both SNR and mMS were related moderately and significantly to IRT, whereas in moderate to advanced glaucoma, mMS was more strongly correlated with IRT than SNR.

Key words: Isolated-check visual evoked potential (icVEP); Primary open-angle glaucoma (POAG); Optical coherence tomography (OCT); Standard automated perimetry (SAP)
https://doi.org/10.1631/jzus.B1900506 **CLC number:** R775

1 Introduction

The underlying cause of glaucomatous damage to retinal structure and function in primary open-angle glaucoma (POAG) appears to be the loss of retinal ganglion cells (RGCs) and their axons (van Buskirk and Cioffi, 1992; Quigley, 1999; Nouri-Mahdavi et al., 2013). Given the basis of typical

‡ Corresponding author
* Project supported by the Wenzhou Medical University (No. QTJ13009), the Health Innovation Talents in Zhejiang Province (2016, No. 25), and the Eye Hospital of Wenzhou Medical University (the Value of Isolated-Check Visual Evoked Potential in Glaucoma Diagnosis and Monitoring), China
ORCID: Li-juan XU, https://orcid.org/0000-0001-6519-3729; Yuan-bo LIANG, https://orcid.org/0000-0001-9685-7356

pathophysiological processes, it is expected that structure and function should be related over the course of the disease. Previous studies in glaucoma, however, demonstrated a weak correlation between them (Harwerth et al., 2007, 2010; Hood et al., 2007, 2013). However, the focus of these visual field (VF) and optical coherence tomography (OCT) studies was primarily on the whole posterior pole rather than the macular area (i.e., peripapillary retinal nerve fiber layer thickness (pRNFLT) vs. ganglion cell layer+inner plexiform layer thickness (GCL+IPLT), 30° vs. 10° VF). According to the studies by Quigley et al. (1989) and Curcio and Allen (1990), nearly 50% of RGCs are concentrated within 4.5 mm of the fovea. The ganglion cell layer and inner plexiform layer (GCL+IPL) include the RGC bodies and dendrites located in the macular region, whereas the retinal nerve fiber layer (RNFL) includes the axons originating in other regions of the retina. Thus, GCL+IPLT might reflect macular structural damage better than pRNFLT. Both isolated-check visual evoked potential (icVEP) and mean macular sensitivity (mMS) applied in this study focus on the macular area and the former is a novel and objective electrophysiological tool that targets the magnocellular pathway of cortical activity, which is selectively damaged in early stage of glaucoma (Zemon et al., 2008; Xu et al., 2017). The latter one, mMS, is recommended for application in glaucoma detection to improve the underestimation of current glaucoma staging systems based on 24-2 (or 30-2) VFs (de Moraes et al., 2019). However, the question as to which is better at reflecting glaucomatous functional damage remains unknown, and therefore, further research is required.

The aim of the current study is to evaluate the relationship between macular functional and structural measures by analyzing the associations between icVEP signal-to-noise ratio (SNR)/mMS and OCT (GCL+IPLT)/pRNFLT with different glaucoma severities, and then to determine which of these measures is a more sensitive indicator of macular changes. To the best of our knowledge, this has not been addressed previously.

2 Subjects and methods

2.1 Subjects

Participants attending the Eye Hospital of Wenzhou Medical University, Wenzhou, China during December 2014 and May 2015 who met the specific inclusion criteria were enrolled in this study. All participants underwent further examinations, including best corrected visual acuity (BCVA; decimal), intraocular pressure (IOP) by Goldmann applanation tonometry, slit-lamp examination, central corneal thickness (CCT) by Lenstar (LENSTAR 900, Haag-Streit AG, Switzerland), gonioscopy (GOLDMANN 905, Haag-Streit AG, Switzerland), spectral domain-OCT (SD-OCT) imaging (Cirrus, Zeiss, Dublin, CA, USA), and fundus photo (VISUCAM 200, Carl Zeiss Meditec, Inc., Jena, Germany). Two reliable standard automated perimetry (SAP; Humphrey Field Analyzer 750i, Carl Zeiss Meditec, Inc., Dublin, CA, USA) tests were performed and the second result was used for analysis. IcVEP (MKWHAMD, CN-V1.4, Huzhou Medconova Medical Technology Co., Ltd., Huzhou, China) was performed as previously described (Xu et al., 2017).

The inclusion criteria for the participants were spherical equivalent between +3.00 and −6.00 D with a cylinder correction within ±3.00 D and a BCVA better than 0.5, no intraocular surgery history within six months, no retinal disease other than POAG, opened anterior chamber angle, reliable SAP results with fixation loss of <20%, both false positive and negative errors less than 15%, and reliable icVEP results. The exclusion criteria for the subjects were: other ophthalmic or neurological conditions that could result in VF defects, a history of diabetes, corticosteroid use, secondary glaucoma, and primary angle-closure glaucoma.

The specific inclusion criteria for the controls were: (1) BCVA of 0.8 or better; (2) IOP of 21 mmHg or lower; (3) no IOP elevation history; (4) the presence of normal fundus photo and reliable normal VF results. The controls should also have no history of ocular disease and no previous intraocular or laser surgery. POAG was diagnosed by glaucomatous optic nerve damage and associated glaucomatous VF defect confirmed by two reliable VF examinations. Glaucoma was classified according to Hodapp-Anderson-Parrish (HAP) criteria (Quigley, 1999; Budenz et al., 2002), and the moderate to advanced stages were defined as the more advanced in this study.

2.2 OCT scanning

Cirrus OCT was used to obtain GCL+IPLT and pRNFLT. It was performed after pupil dilation. The ganglion cell analysis (GCA) algorithm (6.0 software version, Zeiss, Germany) used in this study has been

described previously (Mwanza et al., 2011). The annulus (Fig. 1a) has inner vertical and horizontal diameters of 1.0 and 1.2 mm, respectively, and outer vertical and horizontal diameters of 4.0 and 4.8 mm, respectively. The GCA algorithm identified and calculated the combined thickness of the GCL+IPL. The GCL+IPLT measures provided six wedge-shaped sectors and thicknesses of the mean, minimum, superior, and inferior sectors were analyzed in the current study (Fig. 1a). The pRNFLT used was the overall mean thickness of RNFL. Only the results with signal strength of >6 were considered to be reliable.

2.3 Visual field examination

A VF test of automatic projection perimetry with 24-2 mode was used in this study. The macular VF area was defined as the central VF area correlating topographically with the GCA map by Cirrus OCT as reported previously (Kim et al., 2014). As the elliptical GCA sectors cover an approximate horizontal extent of 2.1° to 8.3° from the fovea and an approximate vertical extent of 1.7° to 7.0°, 12 points of macular sensitivity in the corresponding area on 24-2 SAP were selected as shown in Fig. 1b. Accordingly, mMS was expressed in dB at the central 12 points. The mean value of the superior six points was defined as the superior mMS, and the mean value of the inferior six points was defined as the inferior mMS.

2.4 IcVEP testing

IcVEP testing is a promising electrophysiological technique for early glaucoma (EG) detection. This was described in detail in a previous publication (Xu et al., 2017). The stimuli used in the current study were the same as those in the study by Xu et al. (2017) and SNR values at four increasing levels of DOM (8%, 14%, 22%, and 32%) were collected and analyzed. Each participant underwent at least two times of icVEP testing according to the manufacturers' instructions, and the intra-individual comparisons were analyzed. Only results from intra-individual comparisons of the same eye that yielded a match (F<1.68) were considered to be reliable and were used for further analyses. Different response functions from a representative control and glaucoma case are shown in Fig. 2.

2.5 Statistical analysis

Comparisons of demographic and baseline characteristics between healthy controls and the different POAG subgroups were performed using the analysis of variance for continuous variables or *chi*-square test for dichotomy indices. The Pearson correlation coefficient was used to evaluate the relationships between

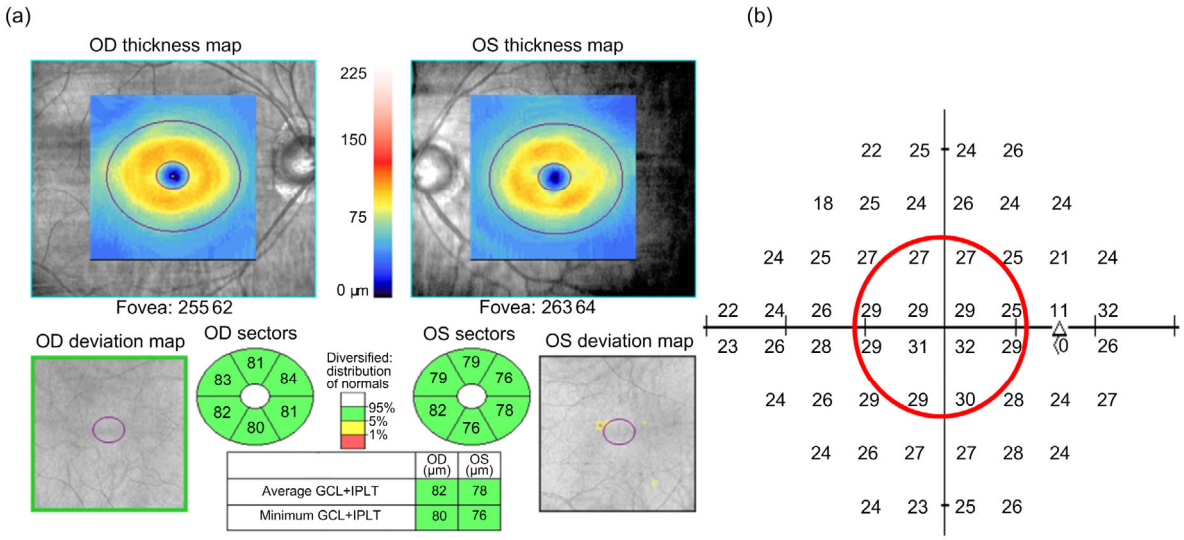

Fig. 1 Structural and functional parameters used in the current study

(a) Ganglion cell layer+inner plexiform layer thickness (GCL+IPLT) map obtained by Cirrus optical coherence tomography (OCT). (b) The central area in the Humphrey 24-2 standard automated perimetry (SAP) showing topographic correlation with the ganglion cell analysis (GCA) map, defined as the macular visual field (VF) area (within the red circle). OD: oculus dexter; OS: oculus sinister

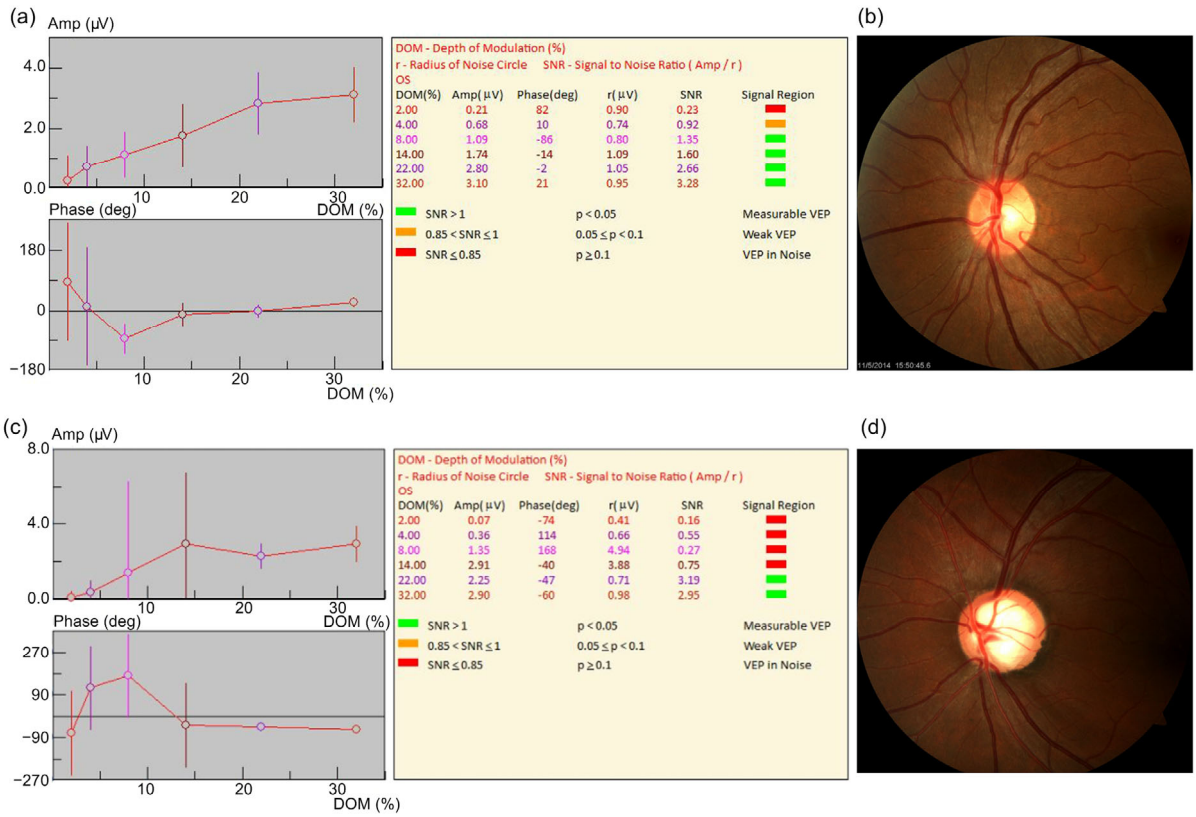

Fig. 2 Representative isolated-check visual evoked potential (icVEP) responses and the correlated fundus photo of a control and a moderate glaucoma patient

(a) IcVEP response of a control; (b) Fundus photo of a control; (c) IcVEP response of a glaucoma patient; (d) Fundus photo of a glaucoma patient. Amp: amplitude; DOM: depth of modulation; SNR: signal-to-noise ratio; VEP: visual evoked potential; OS: oculus sinister

structural and functional parameters. There is no agreed interpretation of the correlation coefficient. In this study, we defined that: $r<0.3$ indicated a weak correlation; $0.3\leq r<0.6$, a moderate correlation; $r\geq 0.6$, a strong correlation. Associations between SNR/mMS and (GCL+IPLT)/pRNFLT were estimated and compared by linear, quadratic, and cubic regression analyses. All statistical analyses were performed using the Statistical Package for the Social Sciences (SPSS) for Windows ver. 20.0 (SPSS Inc., Chicago, IL, USA). $P<0.05$ was used to determine statistical significance.

3 Results

3.1 Subjects

A total of 136 eyes from 136 individuals (60 females, 76 males) were included in the current study, and comprised of 58 healthy controls (38 females, 20 males), 38 EG patients (14 females, 24 males), and 40 moderate to advanced glaucoma (AG) patients (8 females, 32 males). All continuous data were normally distributed in this study. The demographic and clinical characteristics of the control and POAG subgroups are compared in Table 1. There was no age imbalance between groups and a significant difference in gender was observed. All measures of interest (SNR, mMS, GCL+IPLT, and pRNFLT) were negatively correlated with the severity of glaucoma (all $P<0.01$).

3.2 Correlations of structural and functional measurements

Table 2 shows comparisons between SNR/mMS and inner retinal thickness (IRT; including GCL+IPLT and pRNFLT). In EG, there was a significant positive correlation between SNR at 14% DOM and

Table 1 Baseline characteristics of subjects

Group	*n*	Age (year)	Gender (female/male)	Eye (OD/OS)	Spherical equivalent (D)	BCVA	CCT (μm)	IOP (mmHg)
Control	58	47.7±10.2	38/20	37/21	0.1±1.5	1.0±0.1	533.7±27.8	14.5±3.0
EG	38	51.7±13.8	14/24	18/20	−0.3±2.0	0.9±0.2	537.2±31.7	16.9±3.6
AG	40	50.0±13.5	8/32	19/21	−0.9±2.3	0.9±0.2	541.6±35.5	16.3±5.9
P_1		0.127	**0.006**	0.112	0.278	**<0.001**	0.574	**0.001**
P_2		0.344	**<0.001**	0.109	**0.016**	**<0.001**	0.222	0.078
P_3		0.570	0.098	0.991	0.226	0.748	0.568	0.605

Group	SAP			mMS (dB)			SNR	
	MD (dB)	VFI (%)	PSD (dB)	Mean	Superior	Inferior	8% DOM	14% DOM
Control	−1.6±1.3	98.3±1.6	1.8±0.5	31.20±1.20	30.80±1.40	31.50±1.10	1.2±0.5	1.7±0.7
EG	−3.4±1.7	94.3±3.5	3.8±1.8	29.79±1.78	29.32±2.41	30.25±2.38	0.7±0.4	1.0±0.6
AG	−12.0±11.6	62.2±25.7	9.8±3.1	20.70±8.20	18.20±9.90	24.20±8.40	0.6±0.4	0.8±0.6
P_1	**<0.001**	**<0.001**	**<0.001**	**<0.001**	**0.001**	**0.004**	**<0.001**	**<0.001**
P_2	**<0.001**	**<0.001**	**<0.001**	**<0.001**	**<0.001**	**<0.001**	**<0.001**	**<0.001**
P_3	**<0.001**	**<0.001**	**<0.001**	**<0.001**	**<0.001**	**<0.001**	0.358	0.063

Group	SNR		GCL+IPLT (μm)				Mean pRNFLT (μm)
	22% DOM	32% DOM	Mean	Minimal	Superior	Inferior	
Control	2.0±1.1	2.0±0.9	86.1±4.3	82.2±4.9	87.3±4.7	84.9±4.3	98.5±7.9
EG	1.4±0.6	1.6±0.9	74.1±7.0	66.4±9.6	73.1±15.1	73.1±7.3	76.8±12.0
AG	1.2±0.9	1.3±0.9	65.3±10.6	56.4±11.5	66.2±16.7	62.6±9.8	63.8±14.7
P_1	**0.001**	**0.035**	**<0.001**	**<0.001**	**<0.001**	**<0.001**	**<0.001**
P_2	**<0.001**	**<0.001**	**<0.001**	**<0.001**	**<0.001**	**<0.001**	**<0.001**
P_3	0.233	0.116	**<0.001**	**<0.001**	**0.006**	**<0.001**	**<0.001**

Significant differences (P<0.05) are highlighted in bold type. Data (except n) are expressed as mean±standard deviation (SD). P_1: control vs. EG; P_2: control vs. AG; P_3: EG vs. AG. EG: early glaucoma; AG: moderate to advanced glaucoma; OD: oculus dexter; OS: oculus sinister; BCVA: best corrected visual acuity; CCT: central corneal thickness; IOP: intraocular pressure; SAP: standard automated perimetry; MD: mean deviation; VFI: visual field index; PSD: pattern standard deviation; mMS: mean macular sensitivity; SNR: signal-to-noise ratio; DOM: depth of modulation; GCL+IPLT: ganglion cell layer+inner plexiform layer thickness; pRNFLT: peripapillary retinal nerve fiber layer thickness

the inferior GCL+IPLT (r=0.465, P=0.004). In AG, significant positive correlations were found between SNR at 32% DOM and superior GCL+IPLT (r=0.358, P=0.025) and mean GCL+IPLT (r=0.364, P=0.023).

Correlations between mMS and IRT are shown in Table 3. Significant correlations were obtained between them in AG with the r values varying from 0.330 to 0.663 (all P<0.010). In EG, there was significant positive correlation between the mean mMS and minimum GCL+IPLT (r=0.373, P=0.023), and stronger association was found between inferior mMS and superior GCL+IPLT (r=0.470, P=0.003). Correlation models between SNR/mMS and (GCL+IPLT)/pRNFLT were evaluated by regression analysis (Table 4). The structure–function relationship was well explained with a linear model when SNR was plotted against GCL+IPLT. Linear models also explained well the relationship between SNR and pRNFLT. However, the associations between mMS and (GCL+IPLT)/pRNFLT were better explained by nonlinear regression models with higher R^2 values (Fig. 3).

4 Discussion

The purpose of the current study was to investigate associations between central visual function and inner retinal structure, and to determine whether reduced inner macular thickness was reflected in icVEP responses or macular VF loss in POAG patients.

Baseline characteristics of subjects showed that mMS, IRT, and SNR were significantly diminished

Table 2 Correlations between SNR values at different DOMs and sectoral IRT/mMS measures

Group	DOM (%)	GCL+IPLT							
		Mean		Minimum		Superior		Inferior	
		r	*P*	*r*	*P*	*r*	*P*	*r*	*P*
Normal (*n*=58)	8	−0.046	0.732	−0.113	0.398	−0.066	0.623	−0.012	0.931
	14	0.048	0.723	−0.058	0.666	−0.001	0.994	0.090	0.504
	22	0.065	0.628	0.069	0.605	0.024	0.860	0.109	0.415
	32	0.170	0.201	0.082	0.541	0.139	0.297	0.208	0.117
EG (*n*=38)	8	−0.037	0.830	−0.061	0.721	0.015	0.932	−0.083	0.627
	14	0.303	0.068	0.309	0.062	0.084	0.622	**0.465**	**0.004**
	22	0.315	0.058	0.237	0.158	0.313	0.059	0.197	0.242
	32	−0.062	0.714	−0.031	0.857	−0.036	0.832	−0.073	0.669
AG (*n*=40)	8	0.116	0.482	0.195	0.235	0.102	0.538	0.125	0.449
	14	0.002	0.992	−0.058	0.725	−0.036	0.830	0.061	0.711
	22	0.234	0.152	0.142	0.387	0.246	0.131	0.193	0.240
	32	**0.364**	**0.023**	0.227	0.165	**0.358**	**0.025**	0.315	0.051

Group	DOM (%)	pRNFLT		mMS					
		Mean		Minimum		Superior		Inferior	
		r	*P*	*r*	*P*	*r*	*P*	*r*	*P*
Normal (*n*=58)	8	0.178	0.196	−0.100	0.457	−0.076	0.573	−0.117	0.381
	14	0.240	0.081	−0.159	0.233	−0.152	0.254	−0.148	0.269
	22	0.087	0.532	−0.192	0.149	−0.179	0.179	−0.184	0.168
	32	0.216	0.117	−0.091	0.497	−0.122	0.360	−0.040	0.767
EG (*n*=38)	8	0.010	0.956	0.181	0.276	0.233	0.159	0.036	0.831
	14	0.077	0.658	0.076	0.651	0.108	0.520	0.005	0.978
	22	0.123	0.482	**0.326**	**0.046**	0.143	0.391	**0.344**	**0.034**
	32	−0.023	0.895	−0.155	0.352	−0.240	0.147	0.010	0.952
AG (*n*=40)	8	0.057	0.756	0.172	0.290	0.158	0.336	0.271	0.096
	14	0.042	0.821	0.108	0.506	0.099	0.548	0.027	0.872
	22	0.229	0.207	0.299	0.061	0.166	0.313	0.311	0.054
	32	**0.396**	**0.025**	**0.381**	**0.015**	**0.383**	**0.016**	0.262	0.107

Significant differences (P<0.05) are highlighted in bold type. SNR: signal-to-noise ratio; DOM: depth of modulation; IRT: inner retinal thickness; mMS: mean macular sensitivity; EG: early glaucoma; AG: moderate to advanced glaucoma; GCL+IPLT: ganglion cell layer and inner plexiform layer thickness; pRNFLT: peripapillary retinal nerve fiber layer thickness

Table 3 Correlations between sectorial mMS and OCT measures for each group

Group	M-mMS						S-mMS				I-mMS			
	M-GCL+IPLT		Min-GCL+IPLT		M-pRNFLT		S-GCL+IPLT		I-GCL+IPLT		S-GCL+IPLT		I-GCL+IPLT	
	r	*P*	*r*	*P*	*r*	*P*	*r*	*P*	*r*	*P*	*r*	*P*	*r*	*P*
Control (*n*=58)	0.139	0.297	0.195	0.142	0.181	0.190	0.077	0.564	0.055	0.683	0.179	0.179	0.197	0.138
EG (*n*=38)	0.251	0.133	**0.373**	**0.023**	0.215	0.215	0.154	0.361	0.306	0.066	**0.470**	**0.003**	0.019	0.912
AG (*n*=40)	**0.663**	**<0.001**	**0.559**	**<0.001**	**0.561**	**0.001**	**0.464**	**0.003**	**0.624**	**<0.001**	**0.622**	**<0.001**	**0.330**	**0.043**

Significant differences (P<0.05) are highlighted in bold type. EG: early glaucoma; AG: moderate to advanced glaucoma; M: mean; Min: minimum; S: superior; I: inferior; mMS: mean macular sensitivity; OCT: optical coherence tomography; GCL+IPLT: ganglion cell layer+ inner plexiform layer thickness; pRNFLT: peripapillary retinal nerve fiber layer thickness

Table 4 Prediction of SNR/mMS from (GCL+IPLT)/pRNFLT by three polynomial relations (regression curve estimation)

SNR/mMS		IRT	Linear		Quadratic		Cubic	
			R^2	P	R^2	P	R^2	P
SNR	8%	M-GCL+IPLT	0.132	<0.001	0.133	<0.001	0.133	<0.001
	DOM	M-pRNFLT	0.157	<0.001	0.169	<0.001	0.168	<0.001
	14%	M-GCL+IPLT	0.194	<0.001	0.196	<0.001	0.196	<0.001
	DOM	M-pRNFLT	0.221	<0.001	0.236	<0.001	0.236	<0.001
	22%	M-GCL+IPLT	0.149	<0.001	0.150	<0.001	0.151	<0.001
	DOM	M-pRNFLT	0.132	<0.001	0.135	<0.001	0.135	<0.001
	32%	M-GCL+IPLT	0.128	<0.001	0.128	<0.001	0.128	<0.001
	DOM	M-pRNFLT	0.123	<0.001	0.123	<0.001	0.123	<0.001
M-mMS		M-GCL+IPLT	0.532	<0.001	0.646	<0.001	0.646	<0.001
		M-pRNFLT	0.433	<0.001	0.561	<0.001	0.561	<0.001

Data from all groups were combined. M: mean; SNR: signal-to-noise ratio; DOM: depth of modulation; mMS: mean macular sensitivity; IRT: inner retinal thickness; GCL+IPLT: ganglion cell layer+inner plexiform layer thickness; pRNFLT: peripapillary retinal nerve fiber layer thickness

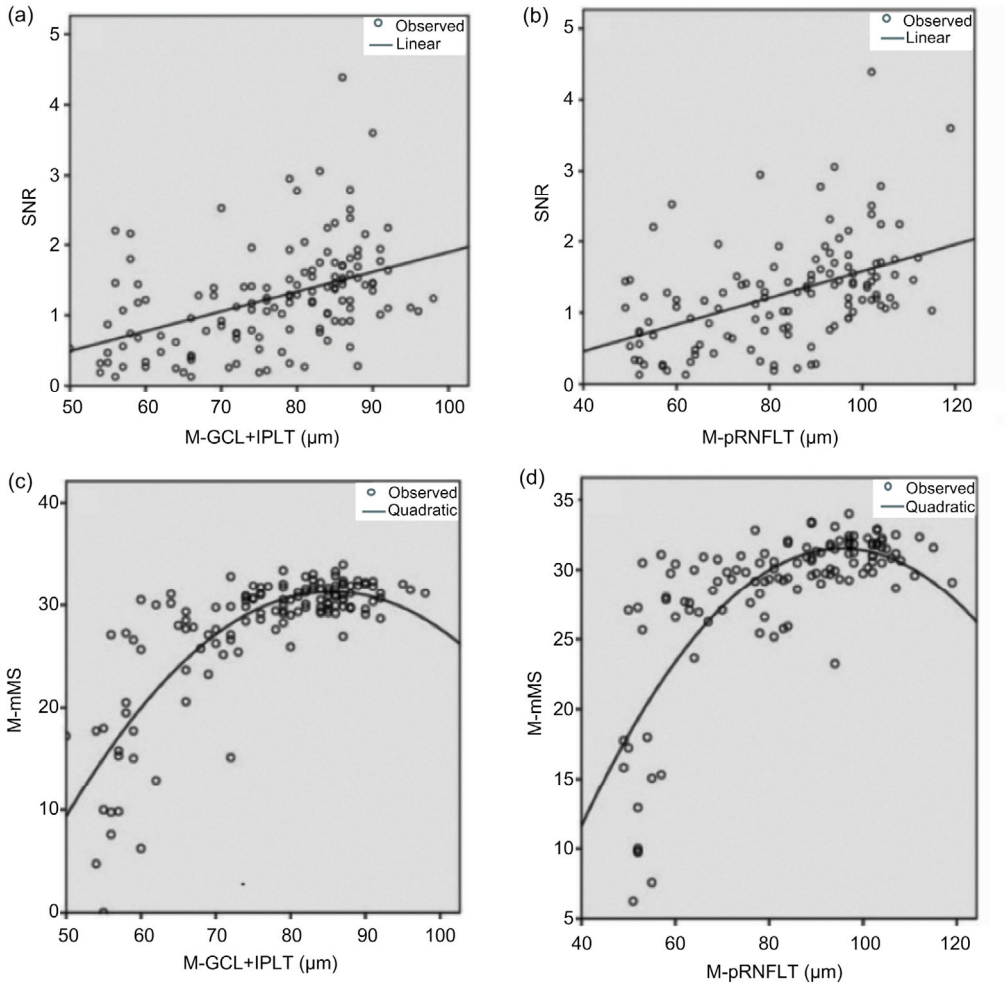

Fig. 3 Scatterplots with model fits of the relationships between SNR/mMS and mean (GCL+IPLT)/pRNFLT
(a) SNR at 14% DOM vs. mean GCL+IPLT: y=−0.909+0.028x. (b) SNR at 14% DOM vs. mean pRNFLT: y=−0.289+0.019x. (c) Mean mMS vs. mean GCL+IPLT: y=−96.037+2.978x−0.017x^2. (d) Mean mMS vs. mean pRNFLT: y=−27.390+1.233x−0.006x^2. M: mean; SNR: signal-to-noise ratio; mMS: mean macular sensitivity; GCL+IPLT: ganglion cell layer+inner plexiform layer thickness; pRNFLT: peripapillary retinal nerve fiber layer thickness

with the severity of glaucoma, indicating damage to the RGCs in the disease process. This study also found a severity-dependent association between SNR/mMS and (GCL+IPLT)/pRNFLT.

The SNR measure from icVEP testing yielded significant correlations with sectors of GCL+IPLT: SNR at 14% DOM with inferior GCL+IPLT in EG, and SNR at 32% DOM with superior GCL+IPLT. A high temporal frequency was used to modulate contrast in the icVEP test. This temporal signal is known to drive M cells strongly; the intent of its use was to target this specific visual pathway. We found that the SNR responses to the four levels of DOM performed differently in correlations with GCL+IPLT. We attribute this finding to the possibly different degrees with which these stimuli drive the different visual pathways. Stimuli with a DOM of 14% might drive large (presumably M) cells to a great extent, which appears to be vulnerable in EG (Glovinsky et al., 1991, 1993; Zemon et al., 1995). By contrast, stimuli with 32% DOM might reflect the responses of small (presumably P) cells, in addition to M cells (Greenstein et al., 1998), both of which are involved in AG.

In the current study, there were significant associations between mean mMS and minimum GCL+IPLT, between inferior mMS and superior GCL+IPLT in EG, and between all observed mMS and matched GCL+IPLT measures in AG. The associations between SNR and GCL+IPLT were moderate in both EG and AG (the highest correlation coefficients of 0.465 and 0.364, respectively); however, those of mMS and GCL+IPLT were comparable in EG (the highest correlation coefficient of 0.470) and generally larger in AG (the highest correlation coefficient of 0.663).

The lack of agreement of these two functional measures in the correlation with structure leads to serious consideration of the underlying mechanisms. These measures reflect different functional aspects of the visual system. According to the theory of "functional reserve," which asserts that a healthy eye has an excess number of RGCs, the VF will remain unchanged until at least 25%–30% of RGCs are lost (Quigley et al., 1989; Bartz-Schmidt et al., 1999; Harwerth et al., 1999; Garway-Heath et al., 2000; Kerrigan-Baumrind et al., 2000). As icVEP detects visual function from RGCs at the cortical level in a "mass response" emphasizing specific visual pathways, it might catch glaucomatous information in an early stage of the disease when VF loss is undetectable. Thus, in the glaucomatous state, icVEP deficits may precede detectable VF defects. However, a somewhat puzzling finding of the current study is that in EG the magnitude of the correlation between SNR as measured by icVEP and GCL+IPLT was not higher than that between mMS and GCL+IPLT. A linear model better explained the correlation between SNR and GCL+IPLT, whereas a quadratic model better explained the association between mMS and GCL+IPLT. We speculate that the decreased mMS detected by VF testing may represent a different kind of glaucomatous damage from that detected by the diminished icVEP SNR. Thus, a combination of these measures may serve to catch more cases of EG.

Another notable finding of the current study is that significant correlations between icVEP SNR and GCL+IPLT were found in certain sectors (inferior GCL+IPLT with SNR at 14% DOM in EG, superior GCL+IPLT with SNR at 32% DOM in AG). These results raise the question of whether specific subsets or regions of RGCs contribute to SNRs at specific DOMs. The amplitude and phase of steady-state VEPs are different in upper vs. lower VF stimulation (Yanashima, 1982), and it is attributed to the different dynamics in the system under these two hemifield conditions (Gutowitz et al., 1986). The inferior GCL+IPL is the macular sector most commonly affected in EG (Hood et al., 2013; Nouri-Mahdavi et al., 2013), and, therefore, its functional role is more impacted at low contrast which drives preferentially the larger RGCs.

As to which structural parameter better reflects macular function, GCL+IPLT or pRNFLT, the results showed that in both EG and AG, certain GCL+IPLT measures yielded significant associations with icVEP SNR. By contrast, a significant association was found only between mean pRNFLT and SNR at 32% DOM in AG. Measures of mMS followed a similar pattern. Unlike studies that treated the entire spectrum of glaucoma patients as a singular group, we focused on subgroups defined by the extent of glaucomatous damage. The current results indicate that GCL+IPLT correlates with macular function well, and in cases of early glaucomatous damage, performs better than pRNFLT.

In light of the above results, the combination of icVEP (especially SNR at 14% DOM), macular VF,

and GCL+IPLT measures is recommended in clinical practice for the early detection of glaucoma. We also propose that icVEP testing (especially SNR at 32% DOM) and GCL+IPLT scanning should be included in the severity evaluation of more advanced glaucoma.

Several limitations of the current study should be considered. Firstly, the design had selection bias. Only Chinese were included in this study, and the role of ethnicity in determining the correlation between structural and functional measures in POAG is unknown. Secondly, the sample size was relatively small, so we were unable to observe any overall age or gender effects. A further study with a larger number of subjects with age and gender matched should be conducted to address this issue. Aiming to better understand the relations between these various measures, further study should focus on follow-up of the structural and functional changes associated with disease progression.

5 Conclusions

In conclusion, the results obtained in the current study revealed a significant severity-dependent association between structural and functional measures. The association was greatest in patients with advanced glaucomatous damage. The results also showed that, for early-stage glaucoma, a similar relationship existed between GCL+IPLT and SNR or mMS. However, for advanced glaucoma, the association between GCL+IPLT and mMS was stronger than that between GCL+IPLT and SNR. Within icVEP measures, SNR at 14% DOM better reflected early glaucomatous damage, and SNR at 32% DOM was superior for advanced glaucoma. In early-stage glaucoma, GCL+IPLT may correlate more strongly with visual function than pRNFLT.

Contributors

Yuan-bo LIANG participated in the conception of the study, analysis of data, revision and final approval of the manuscript. Li-juan XU participated in the design of study, acquisition and analysis of data, drafting of the manuscript and revision, and the final approval of the version. Sha-ling LI participated in the acquisition and analysis of data. Vance ZEMON performed the analysis of data and revision of manuscript. Yan-qian XIE performed the analysis of data. All authors have read and approved the final manuscript. Therefore, the authors have full access to all the data in the study and take responsibility for the integrity and security of the data.

Compliance with ethics guidelines

Li-juan XU, Sha-ling LI, Yan-qian XIE, and Yuan-bo LIANG declare that they have no conflict of interest.

Vance ZEMON, as a principal in VeriSci Corp. (Raritan, NJ, USA), has received a financial interest in Huzhou Medconova Medical Technology Co., Ltd., China.

All procedures followed were in accordance with the ethical standards of the responsible committee on human experimentation (institutional and national) and with the Helsinki Declaration of 1975, as revised in 2008 (5). All participants signed the consent form approved by the Eye Hospital of Wenzhou Medical University, Wenzhou, China.

References

Bartz-Schmidt KU, Thumann G, Jonescu-Cuypers CP, et al., 1999. Quantitative morphologic and functional evaluation of the optic nerve head in chronic open-angle glaucoma. *Surv Ophthalmol*, 44(Suppl 1):S41-S53. https://doi.org/10.1016/S0039-6257(99)00076-4

Budenz DL, Rhee P, Feuer WJ, et al., 2002. Comparison of glaucomatous visual field defects using standard full threshold and Swedish interactive threshold algorithms. *Arch Ophthalmol*, 120(9):1136-1141. https://doi.org/10.1016/j.clinbiochem.2005.11.019

Curcio CA, Allen KA, 1990. Topography of ganglion cells in human retina. *J Comp Neurol*, 300(1):5-25. https://doi.org/10.1002/cne.903000103

de Moraes CG, Sun A, Jarukasetphon R, et al., 2019. Association of macular visual field measurements with glaucoma staging systems. *JAMA Ophthalmol*, 137(2):139-145. https://doi.org/10.1001/jamaophthalmol.2018.5398

Garway-Heath DF, Caprioli J, Fitzke FW, et al., 2000. Scaling the hill of vision: the physiological relationship between light sensitivity and ganglion cell numbers. *Invest Ophthalmol Vis Sci*, 41(7):1774-1782.

Glovinsky Y, Quigley HA, Dunkelberger GR, 1991. Retinal ganglion cell loss is size dependent in experimental glaucoma. *Invest Ophthalmol Vis Sci*, 32(3):484-491.

Glovinsky Y, Quigley HA, Pease ME, 1993. Foveal ganglion cell loss is size dependent in experimental glaucoma. *Invest Ophthalmol Vis Sci*, 34(2):395-400.

Greenstein VC, Seliger S, Zemon V, et al., 1998. Visual evoked potential assessment of the effects of glaucoma on visual subsystems. *Vision Res*, 38(12):1901-1911. https://doi.org/10.1016/S0042-6989(97)00348-9

Gutowitz H, Zemon V, Victor J, et al., 1986. Source geometry and dynamics of the visual evoked potential. *Electroencephalogr Clin Neurophysiol*, 64(4):308-327. https://doi.org/10.1016/0013-4694(86)90155-0

Harwerth RS, Carter-Dawson L, Shen F, et al., 1999. Ganglion cell losses underlying visual field defects from experimental glaucoma. *Invest Ophthalmol Vis Sci*, 40(10):2242-2250.

Harwerth RS, Vilupuru AS, Rangaswamy NV, et al., 2007. The relationship between nerve fiber layer and perimetry measurements. *Invest Ophthalmol Vis Sci*, 48(2):763-773. https://doi.org/10.1167/iovs.06-0688

Harwerth RS, Wheat JL, Fredette MJ, et al., 2010. Linking structure and function in glaucoma. *Prog Retin Eye Res*, 29(4):249-271. https://doi.org/10.1016/j.preteyeres.2010.02.001

Hood DC, Anderson SC, Wall M, et al., 2007. Structure versus function in glaucoma: an application of a linear model. *Invest Ophthalmol Vis Sci*, 48(8):3662-3668. https://doi.org/10.1167/iovs.06-1401

Hood DC, Raza AS, de Moraes CGV, et al., 2013. Glaucomatous damage of the macula. *Prog Retin Eye Res*, 32: 1-21. https://doi.org/10.1016/j.preteyeres.2012.08.003

Kerrigan-Baumrind LA, Quigley HA, Pease ME, et al., 2000. Number of ganglion cells in glaucoma eyes compared with threshold visual field tests in the same persons. *Invest Ophthalmol Vis Sci*, 41(3):741-748.

Kim KE, Park KH, Jeoung JW, et al., 2014. Severity-dependent association between ganglion cell inner plexiform layer thickness and macular mean sensitivity in open-angle glaucoma. *Acta Ophthalmol*, 92(8):e650-e656. https://doi.org/10.1111/aos.12438

Mwanza JC, Oakley JD, Budenz DL, et al., 2011. Macular ganglion cell-inner plexiform layer: automated detection and thickness reproducibility with spectral domain-optical coherence tomography in glaucoma. *Invest Ophthalmol Vis Sci*, 52(11):8323-8329. https://doi.org/10.1167/iovs.11-7962

Nouri-Mahdavi K, Nowroozizadeh S, Nassiri N, et al., 2013. Macular ganglion cell/inner plexiform layer measurements by spectral domain optical coherence tomography for detection of early glaucoma and comparison to retinal nerve fiber layer measurements. *Am J Ophthalmol*, 156(6): 1297-1307.e2. https://doi.org/10.1016/j.ajo.2013.08.001

Quigley HA, 1999. Neuronal death in glaucoma. *Prog Retin Eye Res*, 18(1):39-57. https://doi.org/10.1016/S1350-9462(98)00014-7

Quigley HA, Dunkelberger GR, Green WR, 1989. Retinal ganglion cell atrophy correlated with automated perimetry in human eyes with glaucoma. *Am J Ophthalmol*, 107(5): 453-464. https://doi.org/10.1016/0002-9394(89)90488-1

van Buskirk EM, Cioffi GA, 1992. Glaucomatous optic neuropathy. *Am J Ophthalmol*, 113(4):447-452. https://doi.org/10.1016/s0002-9394(14)76171-9

Xu LJ, Zhang L, Li SL, et al., 2017. Accuracy of isolated-check visual evoked potential technique for diagnosing primary open-angle glaucoma. *Doc Ophthalmol*, 135(2): 107-119. https://doi.org/10.1007/s10633-017-9598-6

Yanashima K, 1982. Surface distribution of steady-state cortical potentials evoked by visual half-field stimulation. *Graefes Arch Clin Exp Ophthalmol*, 218(3):118-123. https://doi.org/10.1007/BF02215648

Zemon V, Eisner W, Gordon J, et al., 1995. Contrast-dependent responses in the human visual system: childhood through adulthood. *Int J Neurosci*, 80(1-4):181-201. https://doi.org/10.3109/00207459508986100

Zemon V, Tsai JC, Forbes M, et al., 2008. Novel electrophysiological instrument for rapid and objective assessment of magnocellular deficits associated with glaucoma. *Doc Ophthalmol*, 117(3):233-243. https://doi.org/10.1007/s10633-008-9129-6

中文概要

题　目：原发性开角型青光眼黄斑区视网膜内层结构和功能的关系

目　的：探讨原发性开角型青光眼（POAG）患者黄斑区视网膜内层结构和功能的关系。

创新点：POAG 的潜在原因是视网膜神经节细胞（RGC）的丢失。虽然在传统上我们可以通过测量视网膜后极部约 30°的结构和功能来评估青光眼性视神经损害，但是 50%的 RGC 存在于黄斑区 4.5 mm 范围内。本研究关注黄斑区约 10°范围视网膜结构和功能的关系，有助于更早地监测到青光眼性视神经损害。

方　法：本研究纳入了 78 例 POAG 患者及 58 例健康对照者，其中 POAG 分为早期青光眼（EG）和中晚期青光眼（AG）。所有受试者均进行了以下检测：分离格栅视觉诱发电位（icVEP）、标准自动视野计（SAP）及光学相干断层扫描（OCT）。icVEP 检测时给予 8%、14%、22%及 32%对比度刺激，采集相应的信躁比（SNR）。黄斑区视野敏感度（mMS）通过计算黄斑中心 12 点的敏感度平均值获得。OCT 扫描包括视网膜神经节细胞层+内丛状层的平均厚度（GCL+IPLT）及视盘周围神经纤维层平均厚度（pRNFLT）。我们比较了各组间 SNR、mMS、GCL+IPLT 及 pRNFLT 值，并分析了结构性指标和功能性指标之间的相关性。

结　论：POAG 组患者的 SNR、mMS、GCL+IPLT 及 pRNFLT 均较正常对照组显著下降（所有 P 值 <0.001）。在早期青光眼中，SNR 及 mMS 均与视网膜内层厚度呈中度相关；而在中晚期青光眼中，mMS 与视网膜内层厚度呈高度相关。

关键词：分离格栅视觉诱发电位（icVEP）；原发性开角型青光眼（POAG）；光学相干断层扫描（OCT）；标准自动视野计（SAP）